

Electromagnetic measurement of the temperature of quark-gluon plasma produced in central ultrarelativistic nuclear collisions

Jean-François Paquet and Steffen A. Bass

Department of Physics, Duke University, Durham, North Carolina 27708-0305, US

(Dated: May 26, 2022)

Ultrarelativistic collisions of large nuclei produce a short-lived plasma of deconfined quarks and gluons. Of all the GeV-energy photons detected in these nuclear collisions, only a small number are emitted directly by the quark-gluon plasma. We use the characteristic near-exponential energy spectrum of these photons to estimate the maximum temperature of the plasma, assuming it undergoes hydrodynamic expansion. We quantify non-exponential corrections to the photon spectrum resulting from the characteristic equation of state and photon emission rate of nuclear matter.

INTRODUCTION

While most photons produced in ultrarelativistic collisions of nuclei are by-products of hadronic decays, a small but measurable number has a more exotic origin: they are emitted directly by quark-gluon plasma, the short-lived plasma of deconfined nuclear matter produced in high-energy nuclear collisions [1–4]. The low-energy spectrum of these non-decay photons has a near exponential dependence [5–9], $\exp(-E/T_{\text{eff}})$. The inverse slope T_{eff} is often interpreted as an “effective temperature” for the plasma. This interpretation of T_{eff} originates from the approximate $[\exp(-E/T)]$ dependence of the photon emission rate, for photons of energy E emitted by a plasma of temperature T .

A large body of work indicates that relativistic fluid dynamics can describe many features of the spacetime evolution of quark-gluon plasma produced in nuclear collisions [10–13]. While the plasma as a whole is globally out of equilibrium, the evidence suggests that one can treat it to a good approximation as being locally close to equilibrium. In this picture, each space-time point in the plasma can be assigned a temperature; this temperature profile is inhomogeneous in space and rapidly varying in time. Because of the complexity of this temperature profile, it has long been understood that the exponential inverse slope T_{eff} of the photon energy spectrum must represent a convoluted average over the plasma’s temperature profile [1, 14]. The interpretation of T_{eff} is further complicated by the plasma’s rapid expansion, which leads to a Doppler blueshift for the produced photons. Finally, the exact rate of photon production by nuclear plasma is highly non-trivial, even assuming a thermalized system [15–28]: while the $[\exp(-E/T)]$ suppression remains the dominant feature of the rate, there are well-known corrections [29].

All the above effects, and more [30], can be included and studied in numerical simulations: hydrodynamics-based models provides realistic temperature and flow velocity profiles for the nuclear plasma, which can be combined with thermal photon production rates [4, 31–38].

In this work, we approach the problem from a dif-

ferent angle. We show that considerable insights can be gained into the factors controlling the photon energy spectrum without numerical simulations [32, 33]. We focus on head-on collisions of large nuclei (“central heavy ion collisions”), which produce quark-gluon plasma with an approximate cylindrical symmetry in the plane transverse to the collision axis. These central collisions have the highest achievable nuclear matter density in collider experiments, increasing the plausibility of the “local equilibrium” assumption. Moreover, the larger number of nucleons participating in the formation of quark-gluon plasma reduces event-by-event fluctuations in the temperature profile of the plasma. This allows for a more meaningful definition of an initial temperature profile, whose maximum is approximately at the center of the nuclear overlap region. In this limit, we find a relation between the photon energy spectrum and this approximate maximum temperature of the plasma.

THERMAL PHOTON ENERGY SPECTRUM AT MIDRAPIDITY

Photon production in collisions of nuclei is described in terms of their momentum perpendicular and parallel to the collision axis. For a photon of momentum K^μ , the rapidity $y_M = \ln[(K^t - K^z)/(K^t + K^z)]/2$ is used as hyperbolic angle to characterize the momentum along the beam axis, with $y_M = 0$ perpendicular to this axis. Cylindrical coordinates are used in the direction orthogonal to the collision axis: k_T and ϕ .

If we focus on photons produced by a locally thermalized plasma, the ϕ -averaged spectrum is given by [39] [40]

$$\frac{1}{2\pi k_T} \frac{dN}{dk_T dy_M} = \int_0^{2\pi} \frac{d\phi}{2\pi} \int \frac{d\tau \tau d^2x d\eta_s}{(\hbar c)^4} \left[k \frac{d\Gamma_\gamma(K \cdot u, T)}{d^3k} \right] \quad (1)$$

where $k d\Gamma_\gamma(K \cdot u, T)/d^3k$ is the rate of production of photons per spacetime volume [15–28]. The temperature and flow velocity profile of the plasma, in space and time, are given respectively by $T(\tau, x, y, \eta_s)$ and $u^\mu(\tau, x, y, \eta_s)$, expressed as a function of the hyperbolic spatial coordi-

nates $\tau^2 = t^2 - z^2$ and $\tanh \eta_s = z/t$.

In collisions of large nuclei, the spacetime region around $\eta_s = 0$ is approximately invariant under longitudinal boosts [41]. In this ‘‘Bjorken’’ longitudinal boost-invariant limit [42], the temperature and transverse flow velocity are independent of η_s , and the η_s -component of the flow velocity can be neglected. Because photons produced at a given *momentum* rapidity y_M originate from a narrow window in *spatial* rapidity η_s around $\eta_s \sim y_M$ [14], one can assume a boost-invariant plasma for photons produced with negligible longitudinal momentum ($y_M \approx 0$). Writing $K \cdot u = k_T \left[\cosh(\eta_s) \sqrt{1 + u_\perp^2} - u_\perp \cos(\phi) \right]$ and using the fact that the dominant momentum dependence of the photon rate is $\exp(-K \cdot u/T)$, integration over η_s and ϕ yields:

$$\frac{1}{2\pi E} \frac{dN}{dEdy_M} \Big|_{y_M=0} \approx \sqrt{2\pi} \int \frac{d\tau \tau d^2x}{(\hbar c)^4} e^{-\frac{Eu_\perp}{T}} I_0 \left(\frac{Eu_\perp}{T} \right) \sqrt{\frac{T}{E\sqrt{1+u_\perp^2}}} \left[k \frac{d\Gamma_\gamma(E(\sqrt{1+u_\perp^2} - u_\perp), T)}{d^3k} \right] \quad (2)$$

where u_\perp and T depend on τ , x and y . The function $I_0(a)$ is the modified Bessel function of the first kind, which can be approximated by $e^{-a} I_0(a) \approx 1/(1+a)$. At $y_M \approx 0$, the transverse momentum k_T of photons corresponds to their energy E , making Eq. 2 truly the energy spectrum of photons. For the rest of the manuscript, we drop the $|_{y_M=0}$ subscript.

TEMPERATURE, VELOCITY AND VOLUME PROFILE OF THE PLASMA

Given the symmetry of head-on nuclear collisions in the plane transverse to the collision axis, we approximate the initial temperature distribution of the plasma as cylindrical. On an event-by-event basis, this symmetry is broken by fluctuations from the quantum nature of nuclear collisions [34, 43]. The width of the initial temperature profile should be approximately the same as the radius of the colliding nuclei, $\sigma_0 \approx 5\text{--}10$ fm for heavy ions such as gold or lead. We use a Gaussian temperature distribution of width σ_0 and maximum temperature $T_{0,\max}$: $T(\tau_0, r) = T_{0,\max} e^{-r^2/(2\sigma_0^2)}$ with $r^2 = x^2 + y^2$. While a Gaussian profile should be a reasonable compromise between accuracy and simplicity, the exact distribution of matter will affect the determination of $T_{0,\max}$; this should be considered a source of uncertainty in the approach.

There is a gradual ramp up of photon production in the early stage of heavy nuclei collisions, as quarks are chemically equilibrating with the initial gluon-dominated medium [44–60]. Eventually the strength of the interactions among quarks and gluons brings them close to local equilibrium. We will assume that the temperature profile is defined at a longitudinal proper time $\tau = \tau_0$. There is

uncertainty in this definition: chemical and thermal equilibrium do not necessarily occur at the same time [61–63], and equilibration may not occur simultaneously across the inhomogeneous plasma. We do not attempt to account for these effects, and assume τ_0 and $T_{0,\max}$ to be defined up to the above uncertainties. To account for the gradual increase in photon emission during chemical equilibration, we approximate photons produced before τ_0 as thermal emission from a temperature profile

$$T(\tau, r) = T(\tau_0, r) (\tau/\tau_0)^\lambda. \quad (3)$$

The parameter λ can be varied to approximate different approaches to equilibrium. Improved treatments that account for non-equilibrium effects should be considered in the future.

For $\tau > \tau_0$, we describe the evolution of the plasma’s temperature and flow velocity profile with inviscid relativistic fluid dynamics. An approximate expression for the transverse flow velocity is [64]

$$u_\perp(\tau, r) \approx \frac{r}{\sigma_0} \frac{\left(\tau - \left(\frac{\tau}{\tau_0} \right)^{c_s^2} \tau_0 \right)}{(1 - c_s^2) \sigma_0 (1 + \tau^2/(2\sigma_0^2))}. \quad (4)$$

where c_s^2 is the speed of sound of the plasma (in units of the speed of light), and we assumed that the *transverse* flow velocity is negligible at time τ_0 . Equation 4 illustrates that, for radius $r \lesssim \sigma_0$, the longitudinal expansion of the plasma dominates over the transverse expansion until $\tau \approx \sigma_0$.

The effect of the transverse flow velocity on the photon spectrum depends on three factors: (i) the magnitude of the transverse flow, (ii) the local effect of transverse flow on photons, and (iii) the origin of the photons that dominates the spectrum at different energies. Equation 4 provides an answer for the first factor: transverse flow is small when $r, (\tau - \tau_0) \ll \sigma_0$, which correspond to the hottest regions of the plasma.

As for the second factor, the local Doppler shift of photons can be estimated from the integrand of Eq. 2. Assuming an exponential emission rate, we expand the integrand at $u_\perp = 0$ and factor out the u_\perp -dependent part, yielding

$$1 + \frac{u_\perp^2}{4} \left[\frac{E}{T} \left(\frac{E}{T} - 2 \right) - 1 \right]. \quad (5)$$

Equation 5 shows that the effect of transverse flow can only be large for $E \gg T$. This effect was discussed and quantified numerically in Refs [32, 33, 65].

Finally, numerical simulations [4, 32, 33, 60, 65, 66] indicate that photons produced at high temperature dominate the photon energy spectrum at high energy ($E \gtrsim 2\text{--}3$ GeV), and photons produced at low temperature dominate at low energy ($E \lesssim 2\text{--}3$ GeV). This is a crucial observation. High temperature regions of the plasma have

small transverse flows (Eq. 4). Photons produced in the lower temperature regions of the plasma (large r and τ), where the transverse flow is large, dominate the lower energy part of the spectrum, where the effect of transverse flow is suppressed (Eq. 5). For these two independent reasons, the effect on photons from the transverse expansion of the plasma is suppressed for both the low and high energy range of the photon spectrum. The effect of the transverse Doppler shift is thus highest at *intermediate* thermal photon energies ($E \approx 2\text{--}3$ GeV), and while not negligible, its effects remain considerably suppressed by the factors discussed above.

The transverse volume of plasma between temperature T_1 and T_2 , defined by [1]

$$V_T(T_1, T_2) = \int d\tau \tau d^2r \Theta(T_1 < T(\tau, r) < T_2) = \int_{T_1}^{T_2} dT \frac{dV_\perp}{dT}$$

can be approximated at times $\tau \lesssim \sigma_0$ by

$$\frac{dV_\perp}{dT} = \frac{\pi \sigma_0^2 \tau_0^2 \left(\left(\frac{T_{0,\max}}{T} \right)^{2c_s^{-2}} - 1 \right)}{T} \quad (6)$$

This formula results from the dominant expansion of the plasma along the beam axis, which yields Bjorken's $T(\tau, r)/T(\tau_0, r) = (\tau_0/\tau)^{c_s^2}$ [42]. Since $2c_s^{-2} \gtrsim 6$, Eq. 6 summarizes that the volume of plasma at a temperature T increases rapidly as T decreases.

Using this transverse volume per unit temperature and neglecting the effect of transverse flow, the photon spectrum (Eq. 2) can be written as

$$\frac{1}{2\pi E} \frac{dN}{dEdy_M} \approx \int_{T_f}^{T_{0,\max}} \frac{dT}{(\hbar c)^4} \frac{dV_\perp}{dT} \sqrt{\frac{2\pi T}{E}} \left[k \frac{d\Gamma_\gamma(E, T)}{d^3k} \right] \quad (7)$$

where $T_{0,\max}$ is the maximum temperature of the plasma, found at time τ_0 , and T_f is a lower bound on the temperature. Guidance for the choice of T_f can be found in studies of the later stage of nuclear collisions, where a transition from fluid dynamics to hadronic transport is necessary given the lower density of nuclear matter. Based on Ref. [67], we can estimate $T_f \approx 120\text{--}140$ MeV, although higher-energy photons do not depend significantly on this value.

For nuclear matter with equal density of baryons and antibaryons, the ratio of speed of sound to the speed of light varies from $\approx 1/7$ at a temperature $T = 170$ MeV, to $1/3$ in the high-temperature limit [68, 69]. Equation 7 can first be solved in the simpler conformal limit, $c_s^2 = \bar{c}_s^2 = 1/3$. We make use of the approximate $T^2 \exp(-E/T)$ temperature dependence of the thermal emission rate $k d\Gamma_\gamma(K \cdot u, T)/d^3k$ [17]. Keeping only the dominant term in $\mathcal{O}(T_f/k_T, T_f/T_{0,\max}, T_{0,\max}/k_T)$ after

integration, we find

$$\frac{1}{2\pi E} \frac{dN}{dEdy_M} \approx \left[\frac{\exp(E/T_{0,\max})}{T_{0,\max}^2} k \frac{d\Gamma_\gamma(E, T_{0,\max})}{d^3k} \right] \frac{\sigma_0^2 \tau_0^2}{(\hbar c)^4} T_{0,\max}^2 e^{-E/T_{0,\max}} \left(\frac{2\pi T_{0,\max}}{E} \right)^{5/2} \bar{c}_s^{-2} \quad (8)$$

To solve Eq. 7 with the temperature-dependent speed of sound of nuclear matter $c_s(T)$, we use the mean value theorem to extract a positive-definite factor

$$\left(\left(\frac{T_{0,\max}}{T^*} \right)^{2c_s^{-2}(T^*)} - 1 \right) / \left(\left(\frac{T_{0,\max}}{T^*} \right)^{2\bar{c}_s^{-2}} - 1 \right) \quad (9)$$

where $T_f < T^*(E) < T_{0,\max}$. Because high-energy *thermal* photons are dominantly produced at high temperature, $\lim_{E \rightarrow \infty} T^*(E) = T_{0,\max}$. We find $T^* \approx T_{0,\max}/(1 + bT_{0,\max}/E)$ with $b = 2$ at $E \gg T_{0,\max}$ [70].

Combining Eq. 8 with the correction factor Eq. 9, we can write the following expression for the logarithm of the photon spectrum, in terms of the initial temperature $T_{0,\max}$, valid for $E \gg T_{0,\max}$:

$$\begin{aligned} \ln \left[\frac{1}{2\pi E} \frac{dN}{dEdy_M} \right] &\approx -E/T_{0,\max} + 5/2 \ln \left(\frac{T_{0,\max}}{E} \right) \\ &+ \ln \left[(2\pi)^{3/2} \frac{\sigma_0^2 \tau_0^2}{(\hbar c)^4} T_{0,\max}^2 \right] + \ln \left[\frac{\exp(E/T_{0,\max})}{T_{0,\max}^2} k \frac{d\Gamma_\gamma(E, T_{0,\max})}{d^3k} \right] \\ &+ 2 \left[c_s^{-2} \left(\frac{T_{0,\max}}{1 + bT_{0,\max}/E} \right) - \bar{c}_s^{-2} \right] \frac{T_{0,\max}}{E} \\ &+ \ln \left(c_s^{-2} \left(\frac{T_{0,\max}}{1 + bT_{0,\max}/E} \right) \right). \quad (10) \end{aligned}$$

In practice, one would want $E \gtrsim 2\text{--}3$ GeV. Recall that Eq. 10 is also approximate because it neglects the effect of the transverse flow velocity.

Equation 10 shows that the dependence of the photon energy spectrum on the maximum temperature $T_{0,\max}$ has significant non-exponential corrections, even in absence of transverse expansion from the plasma. The factor $\ln(T_{0,\max}/E)$ originates from integrating over the power-law increasing spacetime volume of the plasma. The term $\ln [T_{0,\max}^{-2} \exp(E/T_{0,\max}) k d\Gamma_\gamma/d^3k]$ accounts for deviations of the thermal photon emission rate itself from a simple exponential. Finally, deviations from $1/3$ of the speed of sound of nuclear matter lead to a linear term $T_{0,\max}/E$.

If we use the thermal emission rate calculated at leading order in the strong coupling constant g_s , the term $\ln [T_{0,\max}^{-2} \exp(E/T_{0,\max}) k d\Gamma_\gamma/d^3k]$ takes the form [17]:

$$\begin{aligned} \ln \left[\frac{\exp(E/T_{0,\max})}{\exp(E/T_{0,\max}) + 1} \left[\ln \left(\frac{\sqrt{3}}{g_s} \right) + C \left(N_f, \frac{E}{T_{0,\max}} \right) \right] \right] \\ + \ln \left[\alpha_{EM} \left(\sum_{s=1}^{N_f} g_s^2 \right) (N_c^2 - 1) \frac{g_s^2}{4(2\pi)^3} \right] \quad (11) \end{aligned}$$

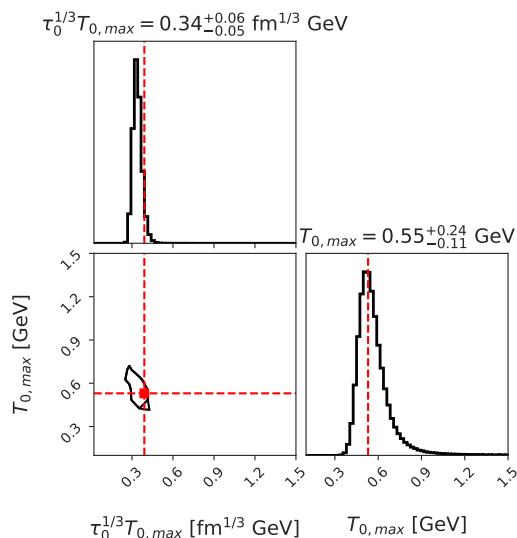


FIG. 1. Posterior constraints (solid black lines) on $\tau_0^{1/3} T_{0,\max}$ and $T_{0,\max}$, comparing Eq. 10 with full numerical calculations of thermal photons from Ref. [60]. The latter used $\tau_0 = 0.4$ fm and $T_{0,\max} \approx 0.53$ GeV [$\tau_0^{1/3} T_{0,\max} = 0.39$ fm $^{1/3}$ GeV], shown as the red dashed lines. The median and 90% credible interval are quoted at the top of the marginalized posteriors.

where $\alpha_{EM} \approx 1/137$ is the electromagnetic coupling constant, q_s is the electric charge of quark species s and $N_c = 3$ is the number of quark colors. Given the plasma's few hundred MeV temperatures, we can ignore photon emission from charm, bottom and top quarks and use three flavors, $N_f = 3$. The function $C(N_f, E/T)$ can be found in Ref. [17].

For photons produced before τ_0 , the same approach can be used, with Eq. 3 instead of the hydrodynamics temperature profile.

To validate Eq. 10, we compare with numerical calculations of thermal photons from Ref. [60]. In these numerical calculations, at $\tau_0 = 0.4$ fm, the initial maximum temperature of the plasma is $T_{0,\max} \approx 0.53$ GeV in Au-Au collisions at $\sqrt{s_{NN}} = 200$ GeV, 0-20% centrality [71]. Using Eq. 10 and pre-equilibrium photons estimated from Eq. 3, we perform a Bayesian parameter inference [72] on the numerical calculations from Ref. [60]. In the Bayesian inference, we fix the equilibration parameter $\lambda \equiv 1$, use Eq. 11 for the photon emission rate, fix the width of the temperature profile to $\sigma_0 = 6$ fm, and assume a 30% “theoretical uncertainty”. We constrain both $T_{0,\max}$ and the product $\tau_0^{1/3} T_{0,\max}$, the latter being an invariant for a conformal plasma dominated by longitudinal hydrodynamic expansion. As shown in Fig. 1, through Eq. 10, we can indeed recover the initial condition parameters from a complex numerical calculation of photon emission. We find that the quasi-invariant $\tau_0^{1/3} T_{0,\max}$ can be constrained more precisely than τ_0 and $T_{0,\max}$ individually.

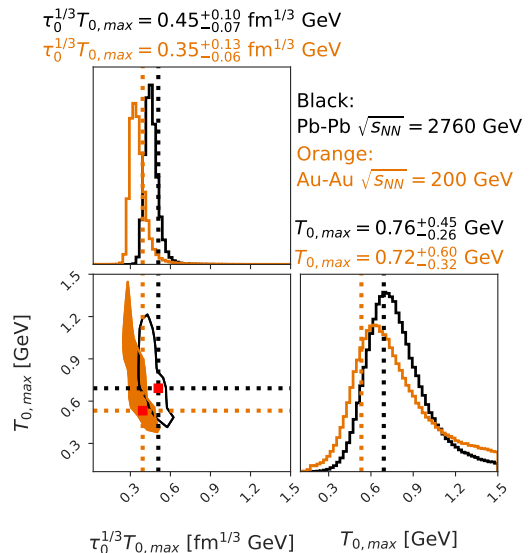


FIG. 2. Posterior constraints on $\tau_0^{1/3} T_{0,\max}$ and $T_{0,\max}$ from comparing Eq. 10 with prompt-subtracted photon spectrum from PHENIX [8] (orange filled contours) and ALICE [6] (black contours). Median and 90% credible interval quoted at the top. The dotted lines and red squares shown for reference are values obtained by comparing numerical multistage models of heavy ion collisions with hadronic measurements [60].

COMPARISON WITH COLLIDER MEASUREMENTS

Available measurements from the Relativistic Heavy Ion Collider and the Large Hadron Collider already subtract hadronic decay photons (e.g. $\pi_0 \rightarrow \gamma\gamma$). An important additional source is the prompt photons, produced in hard interactions of quarks and gluons before the formation of quark-gluon plasma [73, 74]. We subtract these photons using calculations from Ref. [60]. We make the assumption that the three dominant sources of measured photons are decay, prompt and thermal photons. Importantly, we assumed that photon emissions from the quark-gluon plasma can be estimated using equilibrium photon emission rates and ideal fluid dynamics, an approximation that should be revisited.

We compare with RHIC’s PHENIX measurements [8] in Au-Au collisions $\sqrt{s_{NN}} = 200$ GeV, and LHC’s ALICE measurements [6] in Pb-Pb collisions at $\sqrt{s_{NN}} = 2760$ GeV, both for 0–20% centrality. We limit our comparison to measurements with photon energies higher than 2.5 GeV, given the assumptions used to derive Eq. 10. Both PHENIX and ALICE measurements have 20–35% combined statistical and systematic relative uncertainties before subtracting the prompt photons. We assume a conservative 50% uncertainty on the prompt photon calculations [75], yielding a $\gtrsim 40\%$ total uncertainty on the non-prompt non-decay photons [76].

We perform the Bayesian inference as in the previous

section. The results are shown in Fig. 2. The product $\tau_0^{1/3}T_{0,\max}$ is constrained well. For reference, we compare with values of $\tau_0^{1/3}T_{0,\max}$ and $T_{0,\max}$ extracted from state-of-the-art multistage numerical simulations of heavy ion collisions [60]. These results are shown as red squares and dotted lines in Fig 2; they are consistent with the constraints from the present analysis.

The limited constraints on $T_{0,\max}$ reflects the significant uncertainty on current photon spectrum measurements, combined with the uncertainty from subtracting prompt photons.

SUMMARY

We derived expressions relating the energy spectrum of photons measured in central ultrarelativistic nuclear collisions to an approximate maximum temperature of deconfined quark-gluon plasma (Eq. 10). We quantified non-exponential corrections to the photon energy spectrum that are independent of the Doppler shift from the plasma's transverse expansion. These results should inform attempts to extract plasma temperatures from the photon energy spectrum measured in heavy ion collisions, complementing previous numerical studies [32, 33].

In comparisons with measurements, we focused on higher-energy thermal photons, which are less affected by the transverse flow velocity. We found that even a handful of photon spectrum measurements with significant uncertainties can provide constraints on the product $\tau_0^{1/3}T_{0,\max}$, and can estimate the plasma's maximum temperature $T_{0,\max}$ to be larger than 400 MeV at RHIC and 500 MeV at the LHC. These constraints are complementary and consistent with sophisticated numerical simulations of heavy ion collisions, whose constraints originate from hadronic data [77].

An important future direction would be an improved treatment of pre-equilibrium photons and non-equilibrium effects [31, 48, 52, 53, 55–60, 78, 79]. Including corrections from the effect of the transverse flow would further enable comparisons with lower energy photon data.

Acknowledgments This work was supported by the U.S. Department of Energy Grant no. DE-FG02-05ER41367. We thank Mike Sas, Marco Van Leeuwen and the ALICE electromagnetic physics working group for questions and discussions that led to this manuscript. We thank Axel Drees, Charles Gale, Wenqing Fan, Matthew Heffernan, Vladimir Khachatryan, Dananjaya Liyanage, Berndt Müller, Klaus Reygers, Mike Sas, Björn Schenke, Chun Shen and Dinesh Srivastava for discussions and valuable feedback on the manuscript. This research used resources of the National Energy Research Scientific Computing Center (NERSC), a U.S. Department of Energy Office of Science User Facility operated

under Contract No. DE-AC02-05CH11231. We gratefully acknowledge technical support from Rollin Thomas from NERSC.

-
- [1] E. V. Shuryak, Phys. Lett. B **78**, 150 (1978).
 - [2] C. Gale, Landolt-Bornstein **23**, 445 (2010), arXiv:0904.2184 [hep-ph].
 - [3] G. David, Rept. Prog. Phys. **83**, 046301 (2020), arXiv:1907.08893 [nucl-ex].
 - [4] A. Monnai, (2022), arXiv:2203.13208 [nucl-th].
 - [5] A. Adare *et al.* (PHENIX), Phys. Rev. C **91**, 064904 (2015), arXiv:1405.3940 [nucl-ex].
 - [6] J. Adam *et al.* (ALICE), Phys. Lett. B **754**, 235 (2016), arXiv:1509.07324 [nucl-ex].
 - [7] L. Adamczyk *et al.* (STAR), Phys. Lett. B **770**, 451 (2017), arXiv:1607.01447 [nucl-ex].
 - [8] U. A. Acharya *et al.* (PHENIX), (2022), arXiv:2203.17187 [nucl-ex].
 - [9] U. A. Acharya *et al.* (PHENIX), (2022), arXiv:2203.12354 [nucl-ex].
 - [10] C. Gale, S. Jeon, and B. Schenke, Int. J. Mod. Phys. A **28**, 1340011 (2013), arXiv:1301.5893 [nucl-th].
 - [11] U. Heinz and R. Snellings, Ann. Rev. Nucl. Part. Sci. **63**, 123 (2013), arXiv:1301.2826 [nucl-th].
 - [12] E. Shuryak, Rev. Mod. Phys. **89**, 035001 (2017), arXiv:1412.8393 [hep-ph].
 - [13] R. Derradi de Souza, T. Koide, and T. Kodama, Prog. Part. Nucl. Phys. **86**, 35 (2016), arXiv:1506.03863 [nucl-th].
 - [14] L. D. McLerran and T. Toimela, Phys. Rev. D **31**, 545 (1985).
 - [15] J. I. Kapusta, P. Lichard, and D. Seibert, Phys. Rev. D **44**, 2774 (1991), [Erratum: Phys.Rev.D 47, 4171 (1993)].
 - [16] P. Aurenche, F. Gelis, R. Kobes, and H. Zaraket, Phys. Rev. D **58**, 085003 (1998), arXiv:hep-ph/9804224.
 - [17] P. B. Arnold, G. D. Moore, and L. G. Yaffe, JHEP **12**, 009, arXiv:hep-ph/0111107.
 - [18] S. Turbide, R. Rapp, and C. Gale, Phys. Rev. C **69**, 014903 (2004), arXiv:hep-ph/0308085.
 - [19] W. Liu and R. Rapp, Nucl. Phys. A **796**, 101 (2007), arXiv:nucl-th/0604031.
 - [20] K. Dusling and I. Zahed, Phys. Rev. C **82**, 054909 (2010), arXiv:0911.2426 [nucl-th].
 - [21] J. Ghiglieri, J. Hong, A. Kurkela, E. Lu, G. D. Moore, and D. Teaney, JHEP **05**, 010, arXiv:1302.5970 [hep-ph].
 - [22] C. Gale, Y. Hidaka, S. Jeon, S. Lin, J.-F. Paquet, R. D. Pisarski, D. Satow, V. V. Skokov, and G. Vujanovic, Phys. Rev. Lett. **114**, 072301 (2015), arXiv:1409.4778 [hep-ph].
 - [23] C.-H. Lee and I. Zahed, Phys. Rev. C **90**, 025204 (2014), arXiv:1403.1632 [hep-ph].
 - [24] N. P. M. Holt, P. M. Hohler, and R. Rapp, Nucl. Phys. A **945**, 1 (2016), arXiv:1506.09205 [hep-ph].
 - [25] N. P. M. Holt and R. Rapp, Eur. Phys. J. A **56**, 292 (2020), arXiv:2008.00116 [hep-ph].
 - [26] Y. Hidaka, S. Lin, R. D. Pisarski, and D. Satow, JHEP **10**, 005, arXiv:1504.01770 [hep-ph].
 - [27] J. Ghiglieri, O. Kaczmarek, M. Laine, and F. Meyer, Phys. Rev. D **94**, 016005 (2016), arXiv:1604.07544 [hep-lat].

- [28] M. Cè, T. Harris, A. Krasniqi, H. B. Meyer, and C. Török, (2022), arXiv:2205.02821 [hep-lat].
- [29] K. Kajantie and H. I. Miettinen, *Z. Phys. C* **9**, 341 (1981).
- [30] For example, modern numerical simulations include the effect of dissipation in the hydrodynamic description of the fluid, and the corresponding non-equilibrium effects in the photon emission rates [32, 35, 38].
- [31] A. K. Chaudhuri and B. Sinha, *Phys. Rev. C* **83**, 034905 (2011), arXiv:1101.3823 [nucl-th].
- [32] C. Shen, U. W. Heinz, J.-F. Paquet, and C. Gale, *Phys. Rev. C* **89**, 044910 (2014), arXiv:1308.2440 [nucl-th].
- [33] H. van Hees, C. Gale, and R. Rapp, *Phys. Rev. C* **84**, 054906 (2011), arXiv:1108.2131 [hep-ph].
- [34] R. Chatterjee, H. Holopainen, T. Renk, and K. J. Eskola, *Phys. Rev. C* **85**, 064910 (2012), arXiv:1204.2249 [nucl-th].
- [35] J.-F. Paquet, C. Shen, G. S. Denicol, M. Luzum, B. Schenke, S. Jeon, and C. Gale, *Phys. Rev. C* **93**, 044906 (2016), arXiv:1509.06738 [hep-ph].
- [36] Y.-M. Kim, C.-H. Lee, D. Teaney, and I. Zahed, *Phys. Rev. C* **96**, 015201 (2017), arXiv:1610.06213 [nucl-th].
- [37] P. Dasgupta, S. De, R. Chatterjee, and D. K. Srivastava, *Phys. Rev. C* **98**, 024911 (2018), arXiv:1804.02828 [nucl-th].
- [38] O. Garcia-Montero, N. Löhner, A. Mazeliauskas, J. Berges, and K. Reygers, *Phys. Rev. C* **102**, 024915 (2020), arXiv:1909.12246 [hep-ph].
- [39] J. I. Kapusta and C. Gale, *Finite-temperature field theory: Principles and applications*, Cambridge Monographs on Mathematical Physics (Cambridge University Press, 2011).
- [40] The factor $(\hbar c)^4$ assumes that spacetime dimensions are in fermi, and energy and momenta in GeV.
- [41] I. Arsene *et al.* (BRAHMS), *Nucl. Phys. A* **757**, 1 (2005), arXiv:nucl-ex/0410020.
- [42] J. D. Bjorken, *Phys. Rev. D* **27**, 140 (1983).
- [43] M. Dion, J.-F. Paquet, B. Schenke, C. Young, S. Jeon, and C. Gale, *Phys. Rev. C* **84**, 064901 (2011), arXiv:1109.4405 [hep-ph].
- [44] C. T. Traxler and M. H. Thoma, *Phys. Rev. C* **53**, 1348 (1996), arXiv:hep-ph/9507444.
- [45] A. K. Chaudhuri, *J. Phys. G* **26**, 1433 (2000), arXiv:nucl-th/9808074.
- [46] F. Gelis, H. Niemi, P. V. Ruuskanen, and S. S. Rasanen, *J. Phys. G* **30**, S1031 (2004), arXiv:nucl-th/0403040.
- [47] A. Monnai, *Phys. Rev. C* **90**, 021901 (2014), arXiv:1403.4225 [nucl-th].
- [48] L. Bhattacharya, R. Ryblewski, and M. Strickland, *Phys. Rev. D* **93**, 065005 (2016), arXiv:1507.06605 [hep-ph].
- [49] A. Monnai, in *7th International Conference on Hard and Electromagnetic Probes of High-Energy Nuclear Collisions* (2015) arXiv:1510.00539 [nucl-th].
- [50] O. Linnyk, E. L. Bratkovskaya, and W. Cassing, *Prog. Part. Nucl. Phys.* **87**, 50 (2016), arXiv:1512.08126 [nucl-th].
- [51] M. Greif, F. Senzel, H. Kremer, K. Zhou, C. Greiner, and Z. Xu, *Phys. Rev. C* **95**, 054903 (2017), arXiv:1612.05811 [hep-ph].
- [52] V. Vovchenko, I. A. Karpenko, M. I. Gorenstein, L. M. Satarov, I. N. Mishustin, B. Kämpfer, and H. Stoecker, *Phys. Rev. C* **94**, 024906 (2016), arXiv:1604.06346 [nucl-th].
- [53] D. K. Srivastava, R. Chatterjee, and M. G. Mustafa, *J. Phys. G* **45**, 015103 (2018), arXiv:1609.06496 [nucl-th].
- [54] L. Oliva, M. Ruggieri, S. Plumari, F. Scardina, G. X. Peng, and V. Greco, *Phys. Rev. C* **96**, 014914 (2017), arXiv:1703.00116 [nucl-th].
- [55] S. Hauksson, S. Jeon, and C. Gale, *Phys. Rev. C* **97**, 014901 (2018), arXiv:1709.03598 [nucl-th].
- [56] J. Berges, K. Reygers, N. Tanji, and R. Venugopalan, *Phys. Rev. C* **95**, 054904 (2017), arXiv:1701.05064 [nucl-th].
- [57] A. Monnai, *J. Phys. G* **47**, 075105 (2020), arXiv:1907.09266 [nucl-th].
- [58] J. Churchill, L. Yan, S. Jeon, and C. Gale, *Phys. Rev. C* **103**, 024904 (2021), arXiv:2008.02902 [hep-ph].
- [59] O. Garcia-Montero, (2019), arXiv:1909.12294 [hep-ph].
- [60] C. Gale, J.-F. Paquet, B. Schenke, and C. Shen, *Phys. Rev. C* **105**, 014909 (2022), arXiv:2106.11216 [nucl-th].
- [61] A. Kurkela and A. Mazeliauskas, *Phys. Rev. Lett.* **122**, 142301 (2019), arXiv:1811.03040 [hep-ph].
- [62] S. Schlichting and D. Teaney, *Ann. Rev. Nucl. Part. Sci.* **69**, 447 (2019), arXiv:1908.02113 [nucl-th].
- [63] J. Berges, M. P. Heller, A. Mazeliauskas, and R. Venugopalan, *Rev. Mod. Phys.* **93**, 035003 (2021), arXiv:2005.12299 [hep-th].
- [64] A solution of the hydrodynamic equations for $\tau \ll \sigma_0$ yields Eq. 4 without the $1/(1 + \tau^2/(2\sigma_0^2))$. This latter factor can be identified by comparisons with numerical solutions and dimensional analysis.
- [65] J.-F. Paquet, *Nucl. Part. Phys. Proc.* **289-290**, 89 (2017), arXiv:1612.07359 [nucl-th].
- [66] J.-F. Paquet, *Characterizing the non-equilibrium quark-gluon plasma with photons and hadrons*, Ph.D. thesis, McGill U. (2016).
- [67] A. Schäfer, O. Garcia-Montero, J.-F. Paquet, H. Elfner, and C. Gale, (2021), arXiv:2111.13603 [hep-ph].
- [68] S. Borsanyi, Z. Fodor, C. Hoelbling, S. D. Katz, S. Krieg, and K. K. Szabo, *Phys. Lett. B* **730**, 99 (2014), arXiv:1309.5258 [hep-lat].
- [69] A. Bazavov *et al.* (HotQCD), *Phys. Rev. D* **90**, 094503 (2014), arXiv:1407.6387 [hep-lat].
- [70] When E is not much larger than $T_{0,\max}$, numerical results indicate that values closer to $b = 3$ are preferred.
- [71] We used the calculations with IP-Glasma initial conditions and hydrodynamics, but without the initial effective kinetic theory phase (KøMPøST).
- [72] We use a Gaussian likelihood function and flat priors.
- [73] P. Aurenche, M. Fontannaz, J.-P. Guillet, E. Pilon, and M. Werlen, *Phys. Rev. D* **73**, 094007 (2006), arXiv:hep-ph/0602133.
- [74] F. Arleo, K. J. Eskola, H. Paukkunen, and C. A. Salgado, *JHEP* **04**, 055.
- [75] Among others, prompt photons have uncertainties from the nuclear parton distribution function [74, 80–83], the fragmentation function [84–86] as well as effects from partons interacting with quark-gluon plasma [87–90].
- [76] We do not add theoretical uncertainties given the size of the experimental ones.
- [77] In Ref. [60], photons are calculated, but not used to calibrate the multistage simulation.
- [78] B. S. Kasmaei and M. Strickland, *Phys. Rev. D* **102**, 014037 (2020), arXiv:1911.03370 [hep-ph].
- [79] D. Almaalol, A. Kurkela, and M. Strickland, *Phys. Rev. Lett.* **125**, 122302 (2020), arXiv:2004.05195 [hep-ph].
- [80] K. Kovarik *et al.*, *Phys. Rev. D* **93**, 085037 (2016), arXiv:1509.00792 [hep-ph].

- [81] K. J. Eskola, H. Paukkunen, and C. A. Salgado, JHEP **04**, 065, arXiv:0902.4154 [hep-ph].
- [82] K. J. Eskola, P. Paakkinen, H. Paukkunen, and C. A. Salgado, Eur. Phys. J. C **77**, 163 (2017), arXiv:1612.05741 [hep-ph].
- [83] K. J. Eskola, P. Paakkinen, H. Paukkunen, and C. A. Salgado, Eur. Phys. J. C **82**, 413 (2022), arXiv:2112.12462 [hep-ph].
- [84] L. Bourhis, M. Fontannaz, and J. P. Guillet, Eur. Phys. J. C **2**, 529 (1998), arXiv:hep-ph/9704447.
- [85] M. Klasen and F. König, Eur. Phys. J. C **74**, 3009 (2014), arXiv:1403.2290 [hep-ph].
- [86] T. Jezo, M. Klasen, and F. König, JHEP **11**, 033, arXiv:1610.02275 [hep-ph].
- [87] R. J. Fries, B. Muller, and D. K. Srivastava, Phys. Rev. Lett. **90**, 132301 (2003).
- [88] S. Turbide, C. Gale, S. Jeon, and G. D. Moore, Phys. Rev. **C72**, 014906 (2005).
- [89] S. Turbide, C. Gale, E. Frodermann, and U. Heinz, Phys. Rev. **C77**, 024909 (2008).
- [90] B. G. Zakharov, JETP Lett. **80**, 1 (2004), [Pisma Zh. Eksp. Teor. Fiz.80,3(2004)].